Int. J. Electrochem. Sci., 15 **(2020)** 3593 – 3607, doi: 10.20964/2020.04.04

International Journal of ELECTROCHEMICAL SCIENCE
www.electrochemsci.org

Speciation Diagrams in Some Metal Ions-H_3PO_4 System

R. García-García[1*], *G. Orozco*[2], *J. C. Olvera*[2], *J. M. Olivares-Ramírez*[1], *A. Dector.*[3]

[1] Universidad Tecnológica de San Juan del Río, Av. La Palma No. 125, Col. Vista Hermosa, San Juan del Río, Querétaro C. P. 76800, Mexico.
[2] Centro de Investigación y Desarrollo Tecnológico en Electroquímica, Parque Tecnológico. Querétaro, Sanfandila, Pedro Escobedo, C.P. 76703 Querétaro, Mexico.
[3] CONACYT - Universidad Tecnológica de San Juan del Río, Av. La Palma No. 125, Col. Vista Hermosa, San Juan del Río, Querétaro C. P. 76800, Mexico.
[*]E-mail: rgarciag@utsjr.edu.mx

Received: 6 December 2019 / *Accepted:* 18 January 2020 / *Published:* 10 March 2020

There are no substitutes for phosphate rocks as raw materials in the production of phosphate fertilizers and phosphoric acid. We reviewed 222 published articles on purification in which approximately 75% of the studies corresponded to methods of extraction with solvents, methods of precipitation and methods of adsorption. It was estimated that 75-80% of the trace elements present in rocks are not eliminated during the production of phosphoric acid but must be eliminated to obtain purified acid for human use. Speciation diagrams showing that the formation of dimers limits the electrochemical process are presented. Knowledge of the electrical conductivity of phosphoric acid is essential in electrochemistry, and three regions were identified: 1) concentrations lower than 1 mol L^{-1}, where the low conductivity is due to the low concentration of ions; 2) concentrations between 1 mol L^{-1} and 6 mol L^{-1}, where there are more ions and the water-phosphate and phosphate-water-phosphate interactions increase; 3) concentrations higher than 6 mol L^{-1}, where the phosphate-water-phosphate interactions increase further, producing a higher viscosity and greater formation of dimers; consequently, the conductivity decreases and the formation of dimers limits the electrochemical process. Therefore, it is suggested to operate in the second region.

Keywords: Phosphoric acid, Species, Predominance diagrams.

1. INTRODUCTION

Phosphoric acid is widely used as a raw material for the production of fertilizers, foodstuffs, detergents and pharmaceuticals [1]. Fertilizer production from phosphate rock involves heavy metal contaminants and significant carbon emissions. Some phosphate rocks contain thorium and uranium radionuclides and various other heavy metals [2]. Then, if the no purified phosphate rock is applied directly to soils, these metals will be distributed to agricultural soils, risking overexposure to humans

and animals [3–5]. It is clear it will be necessary to address the reduction of heavy metal concentration in phosphate rock, and this topic motivates our study. For it two hundred twenty-two articles describing phosphate purification published from 1974-2019 [6–16] were reviewed, but as techniques are combined in the publications, the techniques were studied 257 times. The above information is presented in Fig. 1.

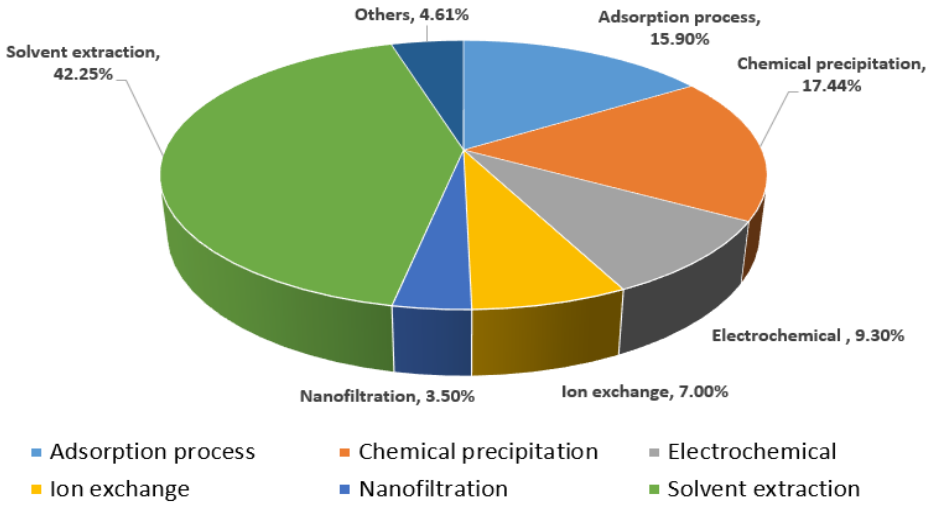

Figure 1. Methods for the purification of phosphoric acid presented in articles published in scientific or technological journals. Several techniques were grouped under the category of other techniques (4.61%) (▬). These techniques are bioleaching (0.39%), crystallization (1.17%), evaporation (0.78%), flotation (0.40%), vertical zone melting (0.77%), reverse osmosis (0.32%), and paramagnetism (0.78%).

The different industrial processes for cadmium removal are from phosphoric acid in wet process (WPA), such as solvent extraction, adsorption, precipitation, ion exchange, flotation and membrane processes, as well as modeling to predict thermodynamic properties, including osmotic coefficient and speciation, are described and analyzed. In addition, the cost and environmental impact of WPA production from the H_3PO_4/H_2O system is presented by Kouzbour [1]. Although speciation diagrams related to electrical conductivity and viscosity were not presented, the formation of dimers was observed during the electrochemical process. Most purification studies do not use electrochemical methods. The most common technique used was solvent extraction (approximately half of the studies), followed by precipitation and adsorption. These three methods represent approximately 75.5% of the published articles, and it is worth mentioning that these techniques are the most used in industry. The percentage of studies focused on the use of membranes (nanofiltration or reverse osmosis) is low (approximately 3.5 and 0.32%, respectively), ion exchange resins are rarely studied (7.0%), and other techniques barely reach 4.61% of the total studies. Electrodialysis, electrocoagulation and electrolysis studies (9.3%) have no industrial use.

No review of electrochemical methods used for phosphoric acid purification was found in the literature; only Scott [17] comments on two electrodialysis (ED) studies conducted around 1995. The traditional application of electrodialysis was to concentrate the reactive-grade acid by a factor of 2-3 times, achieving a concentration of 1.0 mol/dm^3, with an energy consumption of 1.73-2.5 kWh/kg of

P_2O_5. The cost of ED at that time was approximately 17% higher than the cost of evaporation. The process can achieve greater concentration but at the expense of significantly higher energy costs.

Bisang [18] studied the possibility of electrochemically removing arsenic from phosphoric acid. This method uses several electrodes, and the best results were obtained with copper electrodes, where arsenic (As) electrodeposits. It was demonstrated that it is possible to eliminate arsenic with 24% efficiency. The problem of the method is the production of toxic gases during the electrodeposit process.

At high concentrations of mercantile acid, the formation of ionic pairs should be considered, as wet phosphoric acid has a concentration typically ranging from 4 to 6 mol L^{-1}. The formation of polymeric species ($H_5P_2O_8^-$ and $H_6P_2O_8$) at high concentrations, such as 85% by weight [19], has been suggested. Rudolph [20,21] comments that in very dilute solutions of H_3PO_4 at room temperature, there are no bands that can be assigned to these polymeric species and that the product of dissociation, $H_2PO_4^-$ (aq) is the dominant species. The formation of polymeric species can be postulated because the formation of ionic pairs in concentrated aqueous solutions is a commonly observed phenomenon. Initially, it is expected that at high concentrations, ion-ion interactions would predominate over ion-solvent interactions.

Diallo [22] is one of the few researchers who considers in detail the speciation of iron in the presence of phosphates but does not consider the formation of dimers of these phosphates. On the other hand, Koter [23] considers the formation of dimers to create a model of ion transport using the Nernst-Planck equation, but his study does not contain information on the interaction of phosphates with metals such as iron and aluminum, which are the impurities to be eliminated. Dartiguelongue [24] provides a very detailed study of uranium speciation, considering dimers, and its results indicate that complexes are formed without electrical charge, so it would not be advisable to use the electrodialysis technique. After determining speciation, Dartiguelongue [25] performs a solvent extraction study. Studies of the speciation of phosphoric acid indicate the formation of dimeric species, and there is very little information on the interaction of these species with metallic impurities, except for uranium.

Therefore, it is necessary to continue generating information phosphoric acid to improve the operation processes.

2. EXPERIMENTAL PROCEDURE

2.1 Materials and Chemical Products

All reagents were analytical grade and were used without further purification: phosphoric acid (J.T. Baker, 85.4%), sulfuric acid (J.T. Baker, 97.97%). The aqueous solutions were prepared with Milli-Q plus treated water with a resistivity of 11 MΩ cm. All measurements were performed in triplicate.

2.2 Methodology

2.2.1 Viscosity

Viscosity was determined using a Brookfield model LVT viscometer. For the viscosity graphs, 15 measurements were made at different concentrations in percentage by weight (7.5, 15, 20, 30.35, 45,

55, 60, 65, 70, 75, 80, 92, 97.5, 100). The sample was immersed in a 600 ml beaker. The results obtained were in centipoise.

2.2.2 Conductivity

The conductivity was performed using a Fisher Rosemount model 1054B meter with a model 226 toroidal type sensor. The conductivity sensor was immersed in a volume of 2 L of 0.01 M KCl for calibration. Subsequently, measurements were performed at different concentrations in percent by weight (0.0001, 0.0003, 0.001, 0.003, 0.01, 0.03, 0.1, 0.3, 1, 3, 5, 10, 20, 30, 40, 50, 75, 100) and molality (0.1, 0.3, 0.7, 1.0, 2.0, 3.0, 4.0, 5.0, 6.0, 7.0, 8.0, 9.0, 10, 10.7, 13.2, 16.3, 19.98, 24.6, 30 and 38).

Diagrams of the electrical conductivity of phosphoric acid with molarity, molality and concentration expressed in percentage by weight are shown, as well as the variation in the latter with respect to viscosity and analysis and discussion of the variation with the electrical resistance.

Diagrams of predominance of phosphate species are elaborated based on data from tables 1-5 (appendix 1) based on literature [26–32]. Considering the formation of dimeric species with values reported in the literature [27], the degree of dissociation of H_3PO_4($\alpha_{H_3PO_4}$) depending on the concentration of phosphoric acid is explained. The degree of dissociation was calculated based on Cherif [33] from data obtained by Raman spectroscopy. Three regions were identified: concentrations less than 1 mol L^{-1}, concentrations between 1 mol L^{-1} and 6 mol L^{-1} and concentrations greater than 6 mol L^{-1}.

Predominance diagrams are elaborated for monovalent (calcium, magnesium, iron and copper) and trivalent (iron and aluminum) cations. Migration analysis of monovalent, divalent and trivalent (iron and aluminum) metallic species as a function of pH were performed.

3. RESULTS AND DISCUSSION

Fig. 2a-d shows a scenario where ion-ion and solvent-ion interactions change with concentration, being balanced at a maximum concentration of 6.24 molar (Fig. 2a) or 8.99 molal (Fig. 2b) or 50% by weight (Fig. 2c). The electrical conductivity increases when changing from a very dilute concentration to an intermediate concentration (see Fig. 2a-c). This occurs because the number of ions that migrate when an electric field is applied is increased; however, when exceeding 6.24 molar (Fig. 2a), 8.99 molal (Fig. 2b), or 50% by weight (Fig. 2c), the phosphate ions associate with each other, thus increasing viscosity (Fig. 2d) and decreasing the number of free ions that can migrate. Phosphate ions tend to form hydrogen bridges with water, and therefore, this acid has a lower conductivity than other acids. For example, sulfuric acid can have a conductivity 4 times higher than phosphoric acid (Fig. 2c). In highly concentrated acid solutions, the viscosity is very high (Fig. 2d), which will increase the energy cost of the purification process, as the feed pumping will increase. In membrane processes with high concentrations, the filtration or migration efficiencies in the membranes, which are essential parameters that affect the profitability of the process, must be evaluated. The graphs in fig. 2 suggest that

electrodialysis can be performed with a feed concentration of 2.5 mol kg^{-1} to concentrate to 10 mol kg mol^{-1} or at a feed concentration of 20 mol kg^{-1} to dilute to 10 mol kg mol^{-1}.

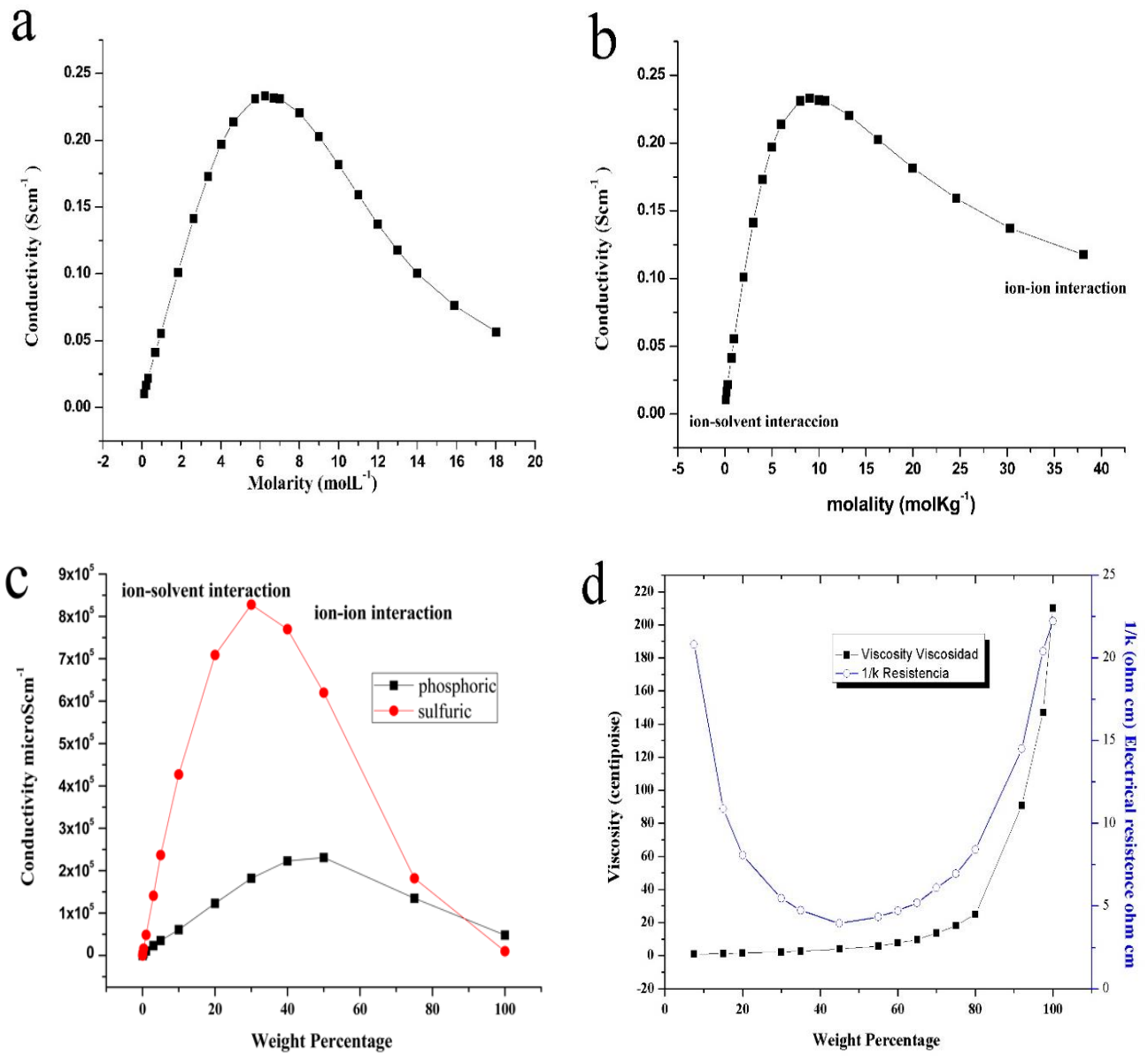

Figure 2. Variation in the electrical conductivity of phosphoric acid with a) molarity, b) molality, c) concentration expressed as a percentage by weight, and d) variation in electrical resistance and viscosity with concentration expressed as a percentage by weight.

Electrical conductivity, density and pH will depend on the concentration of free and associated phosphate ions. In the literature, there are small differences in the reported values with respect to these parameters. For example, Manson [34] reports a molar concentration of 6.2463 mol L^{-1} with a density of 1.3062 g L^{-1}, corresponding to a molality of 8.996 mol kg^{-1}, while Elmore [27] reports a molal concentration of 9.000 mol kg^{-1} corresponding to a molarity of 6.2411 mol L^{-1}.

The formation of high-concentration dimers changes the relationship between the number of water molecules interacting with the solute, thus decreasing the probability that a phosphoric species is in contact with a water molecule [35]. At higher concentrations, the ion-solvent interactions ($H_2PO_4^- \cdot H_2 0$) will be increasingly replaced by ion-ion interactions ($H_2PO_4^- \cdot H_2PO_4^-$). For example, the $H_5P_2O_8^-$ anion was identified at high concentrations by Raman spectroscopy [33,36]. Therefore, the speciation of phosphates will vary, as revealed by the speciation presented in Fig. 3. When dimers are considered in the balance of matter, the H_3PO_4 species has a percentage of 55% at pH 0 (red line in Fig. 3), whereas if dimers are not considered, phosphate would have a concentration of 98% [37,38].

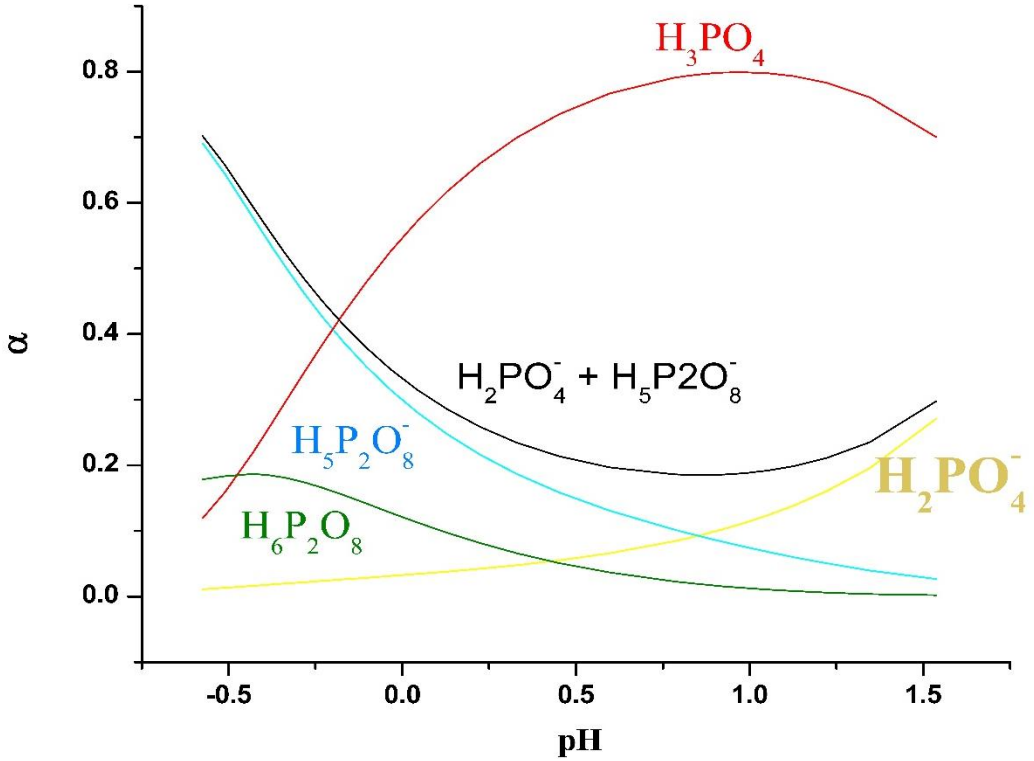

Figure 3. Degree of dissociation of H_3PO_4 at 25°C versus the concentration of phosphoric acid. The degree of dissociation was reported by Elmore [27]. The $\alpha_{H_3PO_4}$ red line (—) considered the formation of a phosphate dimer.

Messnaoui [39] calculates the speciation in the H_3PO_4–H_2O system in the concentration range of 0.1-10 mol kg^{-1}, assuming that dimer formation occurs at that concentration. In his analysis, he finds that the pH is less than 1.7. The result is similar to that observed in fig. 3, and this behavior is explained by Cherif [33] in terms of the formation of dimers with the formula $H_6P_2O_8$ that are later dissociated to produce $H_5P_2O_8^-$; Raman spectroscopy confirms the an interaction between $H_2PO_4^-$ and H_3PO_4 species. The above results indicate that the diagram, shown in the vast majority of textbooks [37], has validity at pH values higher than 1 and phosphate concentrations less than 1 mol kg^{-1}.

Phosphate anions (PO_4^{3-}) are capable of establishing simultaneous bonds with the central atom transition metal, which is considered an impurity in phosphoric acid. Of these complexes, Khalid [30] determines the formation constants of several complexes of Co, Ni, Fe, Ag, Cr and Cu. On the other

hand, the formation of complexes with anions such as $H_5P_2O_8^-$ is rarely reported, except for complexes containing uranium [24], where this phosphate anion must be considered in high concentrations. Therefore, the diagrams reported by Machorro [40] for cations do not show the species actually formed in the acid. It can be speculated that the electrostatic interaction between cation^{n+} and $H_5P_2O_8^-$ or $H_2PO_4^-$ is very intense, and therefore, the cations will migrate into the membranes in the form of phosphate complexes. The formation of these very stable complexes is the key cause of the difficulty of any purification technique. Future research is expected to determine the formation of these complexes by vibration spectroscopy.

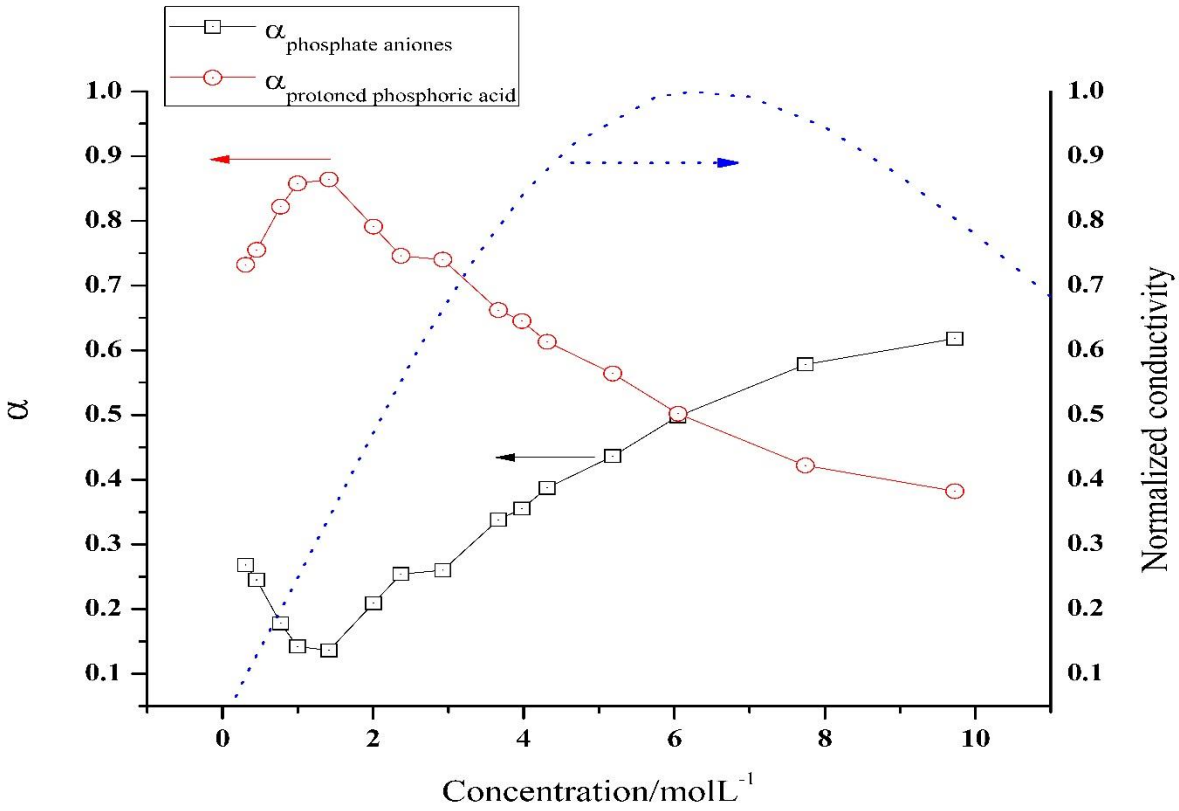

Figure 4. Degree of dissociation of H_3PO_4 ($\alpha_{H_3PO_4}$) versus the concentration of phosphoric acid. The degree of dissociation was calculated based on Cherif [33] from data obtained by Raman spectroscopy at 25°C. The blue line (—) is the conductivity normalized to the maximum as the unit value.

Accordingly, the diagram in textbooks [37] or educational articles [38] cannot identify the species of phosphoric acid in the high concentrations used commercially. Therefore, diagram 4 was constructed considering the formation of dimeric species with the values reported in the literature [33]. It is clear that if these species exclude the concentration of phosphate ions that can migrate, the results will be poorly estimated. For example, if phosphate was not present as an anion (black line with empty boxes in Fig. 4), the observed increase in conductivity would not be explained (blue line in strokes in Fig. 4) when the concentration increased to 6 molL^{-1}. However, although the concentration of ions

increases, the viscosity also increases. This explains the behavior of the graph in Fig. 2d. This type of anion is the most common species of phosphates present at high concentrations. Based on previous paragraphs and Fig. 2, it can be suggested that electrodialysis can be performed with a reference concentration of 10 mol kg mol^{-1} or 6.2 mol L^{-1}.

For concentrated phosphoric acid, due to the formation of dimers, the concentration of H_3PO_4 is almost twice the nominal concentration of phosphoric acid [35]. The graph in Fig. 4 allows us to assume that at a concentration of 6.2 mol L^{-1}, the degree of dissociation of H_3PO_4 is 50%, and the other 50% will consist of $H_6P_2O_8$ (13.52%), $H_2PO_4^-$ (2.95%) and $H_5P_2O_8^{2-}$ (33.52%), as shown in Fig. 3. At a concentration of 9.726 mol L^{-1}, the predominant phosphate species (38.2%, red line) will be the electrically neutral protonated acid (H_3PO_4), and the remaining 61.8% (black line) will consist of other species ($H_6P_2O_8$ (17.4%), $H_2PO_4^-$ (2.3%), $H_5P_2O_8^{2-}$ (42.1%), as shown in Fig. 3). It is worth mentioning that there is some discrepancy between the data in Fig. 3 and Fig. 4 because they were obtained from different studies; however, the values are close.

We consider that the behavior observed in Fig. 4 could be explained by identifying three regions: 1) concentrations lower than 1 mol L^{-1}, where the low conductivity is due to the absence of ions and excessive ion-solvent or water-phosphate interactions; 2) concentrations between 1 mol L^{-1} and 6 mol L^{-1}, where the presence of water molecules still allows the formation of hydrogen bridges, but the phosphate-water-phosphate interactions increase, that is, the ion-ion interaction increases; although electrostatically repulsive in nature, the solvating spheres of the phosphate ions are shared among them, perhaps by means of hydrogen bridges, allowing the existence of anions, which as a whole respond to the electric field to migrate; 3) concentrations greater than 6 mol L^{-1}, which is difficult to explain by considering only coulombic forces, but the viscosity of the medium increases (Fig. 2d); the Stokes equation establishes that ionic mobility is inversely proportional to viscosity, and therefore, in spite the increasing number of anions, each of them is retarded by a mechanical force opposing its movement.

Therefore, electrodialysis should preferably be performed in acidic conditions in the second region by either concentrating or diluting the acid to be in that range of concentrations, since the conductivity is relatively high. In addition, it is important to mention another fact that reinforces operating in the second region, namely, that the viscosity is not as high in region two as in region three, which will also influence the energy expense of pumping to the electrodialysis module.

One possibility to evaluate during the purification of phosphates is leaching of the rock with a base. In this case, it is necessary to know the speciation at pH values higher than 7. There is little information on speciation at high concentrations of phosphate at alkaline pH. At pH values higher than 10, MPO_4^{2-} and $M_2PO_4^-$ [41] complexes, where M is a metal, will preferably be formed. There have been studies of the formation of ion pairs between phosphates, sodium and potassium [42], and at concentrations lower than 0.3 $molkg^{-1}$, several species exist, including $H_2PO_4^-$ ions; however, at concentrations between 0.3 mol kg^{-1} and 0.7 mol kg^{-1}, most of the phosphate forms complexes such as $NaH_2PO_4^-$. At an infinite dilution, the molar conductivities of complexes or ionic pairs of sodium or potassium have been calculated [32], where the concentration of free PO_4^{3-} is 8.2 times greater with potassium ions than with sodium [43]. It is highly probable that cations of transition metals result in significant formation of ionic pairs, as is well determined for sodium and potassium [44].

Water molecules are strongly bound to HPO_4^{2-} and PO_4^{3-} ions at high concentrations, and primary hydration spheres overlap; i.e., water molecules form bridges between these anions [45,46]. Therefore, it can be assumed that cations, water molecules and phosphate anions will have considerable interactions, so the migration will not be of cations but of phosphate-cation complexes, perhaps with their shared hydration spheres. No information was found on the formation of ionic pairs at high concentrations for metals such as aluminum, iron, and copper; however, it is possible to construct speciation graphs considering zero ionic strength. In the case of sodium, complete information on the formation constants of complexes at pH values higher than 12 is not available, as reported by Migneault [47]. However, at pH values lower than 7, the sodium will migrate as a cation, and at pH values higher than 7, it will migrate as an anion. In addition, at a pH of approximately 3, a species will form that has a low tendency to migrate, as it is electrically neutral. Other cations with oxidation state 1^+ will present a similar situation. Metals with an oxidation state of 2^+ will migrate as cations, as shown in Fig. 5, at pH values lower than 4.

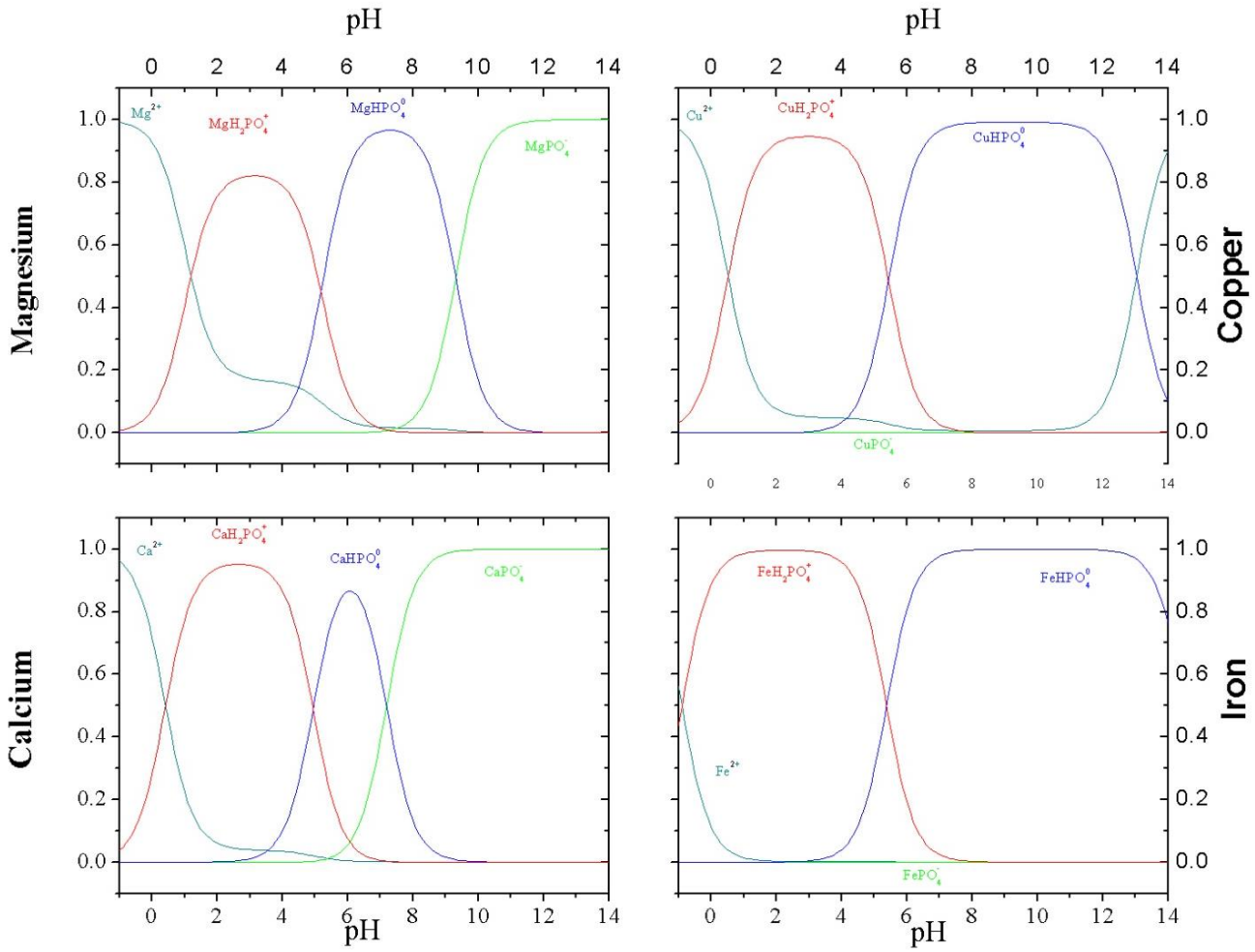

Figure 5. Predominance diagrams for monovalent cations such as calcium, magnesium, iron and copper (Constants in Table 4).

At intermediate pH values, they will form neutral species with little tendency to migrate, and finally, at high pH values, they will form anions and migrate with the free phosphate, as reported by Migneault [47]. Fig. 5 indicates that the purification of metal phosphates with oxidation states of (I) and (II) cannot be performed at very alkaline pH, as both free phosphates and metal-phosphate complexes will be anions and will migrate through an anionic membrane to the same compartment.

The interactions between aluminum and phosphate in aqueous solutions have been notoriously difficult to determine and are rarely studied. For example, the constants reported in Table 5 are among the few that exist, although it is speculated that there are more coordination compounds. In these compounds, a central atom (an aluminum ion with empty valence orbitals) may interact with phosphates that have free electron pairs. These compounds may serve as intermediates for the precipitation of $AlPO_4$ [48]. The existence of negatively or positively charged or neutral coordination compounds is acknowledged [49,50]; however, studies of $AlPO_4$ precipitation or dissolution mechanisms do not consider negatively charged compounds [51,52]. In the case of iron, 14 possible coordination compounds with negative or positive charges have been proposed; however, Fe(III) forms complexes with a positive charge [53–55]. The apparent dissociation constant of iron and aluminum complexes was determined by Mustafa [56], resulting in very close values for iron and aluminum. Fig. 6 shows that metals whose oxidation state is (III) will be able to migrate as cations throughout the pH range.

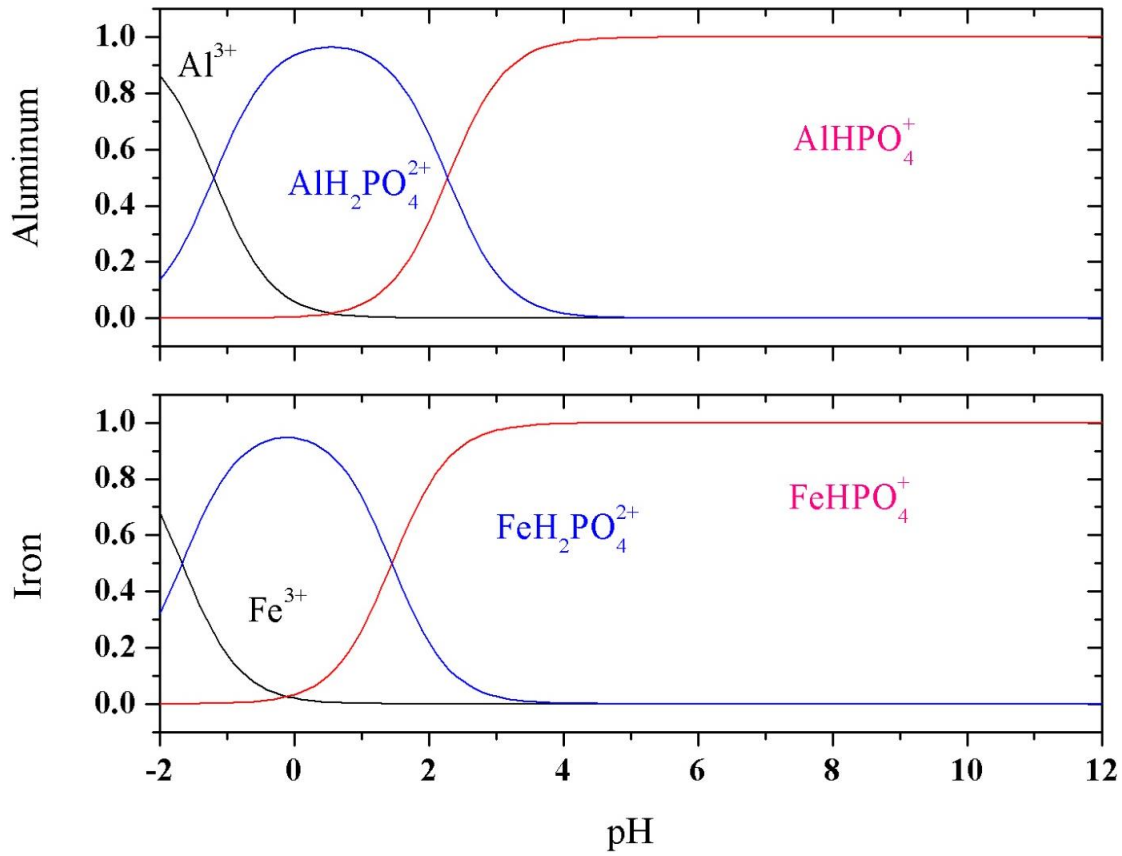

Figure 6. Diagrams of the predominance of trivalent cations such as iron and aluminum. Constants are given in Table 5.

The species diagrams in Figs. 5 and 6 show that separation by electrodialysis will not be efficient at neutral or alkaline pH unless the concentration of the contaminating metals, with an oxidation state of (III), is the highest.

All the graphs are contributions of this work, which will be used in future studies especially in electrodialysis

4. CONCLUSIONS

There is a need to know the speciation of impurities in acids. Thus, speciation diagrams are presented, where it is observed that the formation of dimers limits the electrochemical process. In addition, the phosphate conductivity graphs (Fig. 2) allow us to hypothesize that verifying the conductivity would explain this phenomenon. The main assumption of the possible verification or discrepancy is an follows: If the ion-solvent interaction is carried out by means of phosphate-water-phosphate hydrogen bridges, then when the concentration of phosphates increases, the spheres of solvation will be shared by more phosphate-water-phosphate structures, forming very structured sets that effectively shield the electrostatic repulsion that the anions experience among themselves. It is worth mentioning that this very structured set must balance the attractions and electrostatic repulsions of the anions and protons; then, its structure will be rigid and compact, which explains the high viscosity.

If the hypothesis is fulfilled, the free protons will not vary according to the equilibrium constants given in Table 1 but will correspond to the values in Table 2.

Knowledge of the conductivity of phosphoric acid is essential in electrochemistry. Evaluation of this conductivity clearly indicates that the process of concentration or desalination in electrodialysis should consider a concentration of phosphoric acid of 6 molar as a reference and a pH close to -0.25.

APPENDIX

Tables of equilibrium of phosphate species and their dissociation constants

Table 1. Balance considered in the speciation diagram (3 and 4) with different ionic strengths (I)

Reaction	Constants
$H_3PO_4^0 \leftrightarrow H^+ + H_2PO_4^-$	$K_{H1} = \frac{[H^+][H_2PO_4^-]}{[H_3PO_4^0]}$ I=1, $K_{H1}=10^{-1.70}$; I=0, $K_{H1}=10^{-2.148}$
$H_2PO_4^- \leftrightarrow H^+ + HPO_4^{2-}$	$K_{H2} = \frac{[H^+][HPO_4^{2-}]}{[H_2PO_4^-]}$ I=1, $K_{H2}=10^{-6.46}$, I=0,K_{H2}, $10^{-7.199}$,
$HPO_4^{2-} \leftrightarrow H^+ + PO_4^{3-}$	$K_{H3} = \frac{[H^+][PO_4^{3-}]}{[HPO_4^{2-}]}$ I=1,$K_{H3}=10^{-10.79}$; I=0, $K_{H3}=10^{-12.35}$

Table 2. Balances and formation constants of phosphate dimers. The data were obtained from the mass balance graph presented by Elmore [26].

Reaction	Constants
$H_3PO_4^0 + H_2PO_4^- \leftrightarrow H_5P_2O_8^-$	$K_{4H} = \frac{[H_5P_2O_8^-]}{[H_3PO_4][H_2PO_4^-]} = 1.263$
$H_6P_2O_8^0 \leftrightarrow H^+ + H_5P_2O_8^-$	$K_{5H} = \frac{[H^+][H_5P_2O_8^-]}{[H_6P_2O_8^0]} = 0.3$

Table 3. Balances and dissociation constants of sodium complexes [31]

Reaction	Constants
$NaH_2PO_4^0 \leftrightarrow Na^+ + H_2PO_4^-$	$K_6 = \frac{[Na^+][H_2PO_4^-]}{[NaH_2PO_4^0]} = 10^{0.31}$
$NaHPO_4^- \leftrightarrow Na^+ + HPO_4^{2-}$	$K_7 = \frac{[Na^+][HPO_4^{2-}]}{[NaHPO_4^-]} = 10^{-0.114}$
$NaPO_4^{2-} \leftrightarrow Na^+ + PO_4^{3-}$	$K_8 = \frac{[Na^+][PO_4^{3-}]}{[NaPO_4^{2-}]} = 10^{0.453}$

Table 4. Balances and dissociation constants of divalent cation-phosphate complexes [25,28].

Reaction	Constants
$CaPO_4^- \leftrightarrow Ca^{2+} + PO_4^{3-}$	$K_9 = \frac{[Ca^{2+}][PO_4^{3-}]}{[CaPO_4^-]} = 10^{-6.46}$
$CaHPO_4 \leftrightarrow Ca^{2+} + HPO_4^{2-}$	$K_{10} = \frac{[Ca^{2+}][HPO_4^{2-}]}{[CaHPO_4]} = 10^{-2.74}$
$CaH_2PO_4^+ \leftrightarrow Ca^{2+} + H_2PO_4^-$	$K_{11} = \frac{[Ca^{2+}][H_2PO_4^-]}{[CaH_2PO_4^+]} = 10^{-1.4}$
$MgPO_4^- \leftrightarrow Mg^{2+} + PO_4^{3-}$	$K_{12} = \frac{[Mg^{2+}][PO_4^{3-}]}{[MgPO_4^-]} = 10^{-6.43}$
$MgHPO_4 \leftrightarrow Mg^{2+} + HPO_4^{2-}$	$K_{13} = \frac{[Mg^{2+}][HPO_4^{2-}]}{[MgHPO_4]} = 10^{-3.08}$
$MgH_2PO_4^+ \leftrightarrow Mg^{2+} + H_2PO_4^-$	$K_{14} = \frac{[Mg^{2+}][H_2PO_4^-]}{[MgH_2PO_4^+]} = 10^{-1.38}$
$CuPO_4^- \leftrightarrow Cu^{2+} + PO_4^{3-}$	$K_{15} = \frac{[Cu^{2+}][PO_4^{3-}]}{[CuPO_4^-]} = 10^{6}$
$CuHPO_4 \leftrightarrow Cu^{2+} + HPO_4^{2-}$	$K_{16} = \frac{[Cu^{2+}][HPO_4^{2-}]}{[CuHPO_4]} = 10^{-2.14}$

$CuH_2PO_4^+ \leftrightarrow Cu^{2+} + H_2PO_4^-$	$K_{17} = \frac{[Cu^{2+}][H_2PO_4^-]}{[CuH_2PO_4^+]} = 10^{-1.3}$
$FePO_4^- \leftrightarrow Fe^{2+} + PO_4^{3-}$	$K_{18} = \frac{[Fe^{2+}][PO_4^{3-}]}{[FePO_4^-]} = 10^{6}$
$FeHPO_4 \leftrightarrow Fe^{2+} + HPO_4^{2-}$	$K_{19} = \frac{[Fe^{2+}][HPO_4^{2-}]}{[FeHPO_4]} = 10^{-3.6}$
$FeH_2PO_4^+ \leftrightarrow Fe^{2+} + H_2PO_4^-$	$K_{20} = \frac{[Fe^{2+}][H_2PO_4^-]}{[FeH_2PO_4^+]} = 10^{-2.7}$

Table 5. Balances and dissociation constants of trivalent cation-phosphate complexes [25, 28-30].

Reaction	Constants
$AlHPO_4^+ \leftrightarrow Al^{3+} + HPO_4^{2-}$	$K_{21} = \frac{[Al^{3+}][HPO_4^{2-}]}{[AlHPO_4^+]} = 10^{-7}$
$AlH_2PO_4^{2+} \leftrightarrow Al^{3+} + H_2PO_4^-$	$K_{22} = \frac{[Al^{3+}][H_2PO_4^-]}{[AlH_2PO_4^{2+}]} = 10^{-3}$
$FeHPO_4^+ \leftrightarrow Fe^{3+} + HPO_4^{2-}$	$K_{23} = \frac{[Fe^{3+}][HPO_4^{2-}]}{[FeHPO_4^+]} = 10^{-7}$
$FeH_2PO_4^{2+} \leftrightarrow Fe^{3+} + H_2PO_4^-$	$K_{24} = \frac{[Fe^{3+}][H_2PO_4^-]}{[FeH_2PO_4^{2+}]} = 10^{-3}$

Rererences

1. S. Kouzbour, B. Gourich, F. Gros, C. Vial, F. Allam, Y. Stiriba, *Hydrometallurgy*, 188 (2019) 222–247.
2. F.T. da Conceição, M.L.P. Antunes, S.F. Durrant, *Environ. Geochem. Health*, 34 (2012) 103–111.
3. K.F. Isherwood, Proc. an Int. Work. Curr. Environ. Issues Fertil. Prod., (1998) Paris, pp. 164–167.
4. Y. Liu, G. Villalba, R.U. Ayres, H. Schroder, *J. Ind. Ecol.*, 12 (2008) 229–247.
5. G. Villalba, Y. Liu, H. Schroder, R.U. Ayres, *J. Ind. Ecol.*, 12 (2008) 557–569.
6. M.F. Rodríguez Ordoñez, Estudio Virtual de Un Reactor Electroquímico y Su Perspectiva Para La Purificación de Efluentes Con Fosfatos, Tesis de Maestría, cideteq México , 2018.
7. G. Allaedini, P. Zhang, *Int. J. Surf. Eng. Interdiscip. Mater. Sci.*, 7 (2019) 1–18.
8. (2019).
9. E.M. El Gammal, S.H. Ahmed, *J. Radioanal. Nucl. Chem.*, (2019) (in press)
10. B. Khoualdia, M. Loungou, E. Elaloui, *Http://Www.Sciencepublishinggroup.Com.*, 3 (2019) 83.
11. M.M. Ali, A.A. Attia, M.H. Taha, M.M. El-Maadawy, A.M. Abo-Raia, A. Abouria, SPE Middle East Oil Gas Show Conf., Society of Petroleum Engineers, (2019).
12. H. Barrak, R. Ahmedi, P. Chevallier, A. M'nif, G. Laroche, A.H. Hamzaoui, *Sep. Purif. Technol.*, 222 (2019) 145–151.
13. M.I. Amin, H.S. Gado, W.M. Youssef, A.M. Masoud, *Chem. Pap.*, 73 (2019) 1871–1877.

14. X. Leng, Y. Zhong, D. Xu, X. Wang, L. Yang, *Chinese J. Chem. Eng.*, 27 (2019) 1050–1057.
15. H.M. Abdel-Ghafar, E.A. Abdel-Aal, M.A.M. Ibrahim, H. El-Shall, A.K. Ismail, *Hydrometallurgy*, 184 (2019) 1–8.
16. J. Zieliński, M. Huculak-Mączka, M. Kaniewski, D. Nieweś, K. Hoffmann, J. Hoffmann, *Hydrometallurgy*, 190 (2019) 105157.
17. K. (Keith) Scott, Handbook of Industrial Membranes, Elsevier Advanced Technology, (1995).
18. J.M. Bisang, F. Bogado, M.O. Rivera, O.L. Dorbessan, *J. Appl. Electrochem.*, 34 (2004) 375–381.
19. G. Ferroni, *Electrochim. Acta*, 21 (1976) 283–286.
20. W.W. Rudolph, *Dalt. Trans.*, 39 (2010) 9642–9653.
21. W.W. Rudolph, *J. Solution Chem.*, 41 (2012) 630–645.
22. H. Diallo, M. Rabiller-Baudry, K. Khaless, B. Chaufer, *J. Memb. Sci.*, 427 (2013) 37–47.
23. S. Koter, M. Kultys, *Sep. Purif. Technol.*, 73 (2010) 219–229.
24. A. Dartiguelongue, E. Provost, A. Chagnes, G. Cote, W. Fürst, *Solvent Extr. Ion Exch.*, 34 (2016) 241–259.
25. A. Dartiguelongue, A. Chagnes, E. Provost, W. Fürst, G. Cote, *Hydrometallurgy*, 165 (2016) 57–63.
26. by Robert M. Smith, and Arthur E. Martell, CRITICAL STABILITY CONSTANTS Volume 4: Inorganic Complexes, 1 st edition, Plenum Press, New York, (1976).
27. K.L. Elmore, J.D. Hatfield, R.L. Dunn, A.D. Jones, *J. Phys. Chem.*, 69 (1965) 3520–3525.
28. C.F. Weber, E.C. Beahm, J.S. Watson, *J. Solution Chem.*, 28 (1999) 1207–1238.
29. M. Hanhoun, L. Montastruc, C. Azzaro-Pantel, B. Biscans, M. Frèche, L. Pibouleau, *Chem. Eng. J.*, 167 (2011) 50–58.
30. K. Abu-Shandi, F. Al-Wedian, *Chem. Pap.*, 63 (2009) 420–425.
31. H.L. Bohn, M. Peech, *Soil Sci. Soc. Am. J.*, 33 (1969) 873–876.
32. A.D. Pethybridge, J.D.R. Talbot, W.A. House, *J. Solution Chem.*, 35 (2006) 381–393.
33. M. Cherif, A. Mgaidi, N. Ammar, G. Vallée, W. Fürst, *J. Solution Chem.*, 29 (2000) 255–269.
34. C.M. Mason, J.B. Culvern, *J. Am. Chem. Soc.*, 71 (1949) 2387–2393.
35. J. Ma, U. Schmidhammer, M. Mostafavi, *J. Phys. Chem. B*, 119 (2015) 7180–7185.
36. M. Cherif, A. Mgaidi, M.N. Ammar, M. Abderrabba, W. Fürst, *Fluid Phase Equilib.*, 175 (2000) 197–212.
37. G. Trejo Córdova, A. Rojas Hernández, M.T. Ramírez Silva, Diagramas de Zonas de Predominio Aplicados Al Análisis Químico, UAM, Iztapalapa, (1993) México.
38. R. Moya-Hernández, J.C. Rueda-Jackson, J. Havel, M.T. Ramírez, G.A. Vázquez, A. Rojas-Hernández, *J. Chem. Educ.*, 79 (2002) 389.
39. B. Messnaoui, T. Bounahmidi, *Fluid Phase Equilib.*, 237 (2005) 77–85.
40. J.J. Machorro, J.C. Olvera, A. Larios, H.M. Hernández-Hernández, M.E. Alcantara-Garduño, G. Orozco, *ISRN Electrochem.*, 2013 (2013) 1–12.
41. P.G. Daniele, A. De Robertis, C. De Stefano, A. Gianguzza, S. Sammartano, *J. Solution Chem.*, 20 (1991) 495–515.
42. H. Bianchi, P.R. Tremaine, *J. Solution Chem.*, 24 (1995) 439–463.
43. C.M. Preston, W.A. Adams, *J. Phys. Chem.*, 83 (1979) 814–821.
44. G.E. Woolston, L.N. Trevani, P.R. Tremaine, *J. Chem. Eng. Data*, 53 (2008) 1728–1737.
45. E. Pluhařová, M. Ončák, R. Seidel, C. Schroeder, W. Schroeder, B. Winter, S.E. Bradforth, P. Jungwirth, P. Slavíček, *J. Phys. Chem. B*, 116 (2012) 13254–13264.
46. A. Eiberweiser, A. Nazet, G. Hefter, R. Buchner, *J. Phys. Chem. B*, 119 (2015) 5270–5281.
47. D.R. Migneault, R.K. Forc, *J. Solution Chem.*, 17 (1988) 987–997.
48. R.E. White, L.O. Tiffin, A.W. Taylor, *Plant Soil*, 45 (1976) 521–529.
49. J.E. Salmon, J.G.L. Wall, *J. Chem. Soc.* (1958) 1128–1134.
50. L.R.F.J. and J.E.S. R. E. White, *J. Chem. Soc.*, (1954) 4013–4017.

51. F. Lagno, G.P. Demopoulos, *Environ. Technol.*, 27 (2006) 1217–24.
52. L.S. Burrell, C.T. Johnston, D. Schulze, J. Klein, J.L. White, S.L. Hem, *Vaccine*, 19 (2000) 275–281.
53. A. V. Kuzin, I.G. Gorichev, Y.A. Lainer, *Russ. Metall.*, 2013 (2013) 652–657.
54. R.B. Wilhelmy, R.C. Patel, E. Matijevic, *Inorg. Chem.*, 24 (1985) 3290–3297.
55. K. Kandori, T. Kuwae, T. Ishikawa, *J. Colloid Interface Sci.*, 300 (2006) 225–31.
56. S. Mustafa, A. Naeem, S. Murtaza, N. Rehana, H.. Samad, *J. Colloid Interface Sci.*, 220 (1999) 63–74.